Original Article

Types and Metallogenic Mechanism of Rubidium Deposits in Mainland China

Jian Zhao Yin[1] Ⓛ

Abstract

Mainland China holds a dominant global position in terms of rubidium resources; while rubidium mineralization of various types has been discovered across many regions, most occurrences are low-grade associated/paragenetic deposits that are difficult to develop and process. Genetically, the country's known rubidium deposits fall into three categories: endogenic, exogenic, and those formed by the superposition of endogenic and exogenic processes. The endogenic category encompasses types such as pegmatites (broadly defined), granites (broadly defined), magmatic-hydrothermal systems, crypto-explosive breccias, alkaline igneous rocks, porphyries, skarns, and volcanic rocks. Deposits formed by the superposition of endogenic and exogenic mineralizations include brines, Quaternary hot springs, and coal-hosted deposits. Exogenic deposits consist of weathered granite crusts and minor placer-type occurrences. Rubidium mineralization is closely linked to tectono-magmatic activity. Key ore-controlling factors include, but are not limited to: magmatic fractional crystallization and hydrothermal metasomatism; the degree of magmatic differentiation; the intensity of magma melt-fluid interaction and crustal contamination; oxygen fugacity and the remelting of crustal material; alteration intensity; the involvement of fluxing and incompatible elements; and the influx of mantle-derived material (including its quantity and/or extent). For liquid-phase deposits—specifically brine types—additional ore-controlling factors include hot spring temperatures, etc.

Keywords: genetic type; geology; rubidium deposits; endogenic/exogenic type; type formed by the superposition of endogenic and exogenic geological processes; mainland China

---

Affiliation Info: 1 College of Earth Sciences, Jilin University, Changchun 130061, China

Corresponding AurhorⓁ: Yin, J. Z., PhD, Professor, geosciences, mineral exploration and mining; Email address: jzyin7@jlu.edu.cn

Citation: Yin, J.Z. 2026. Types and metallogenic mechanism of rubidium deposits in Mainland China. *Naturalis Scientias*, 3: 777-802. DOI: https://doi.org/10.62252/NSS.2026.1043. www.naturalisscientias.com.

Copyright © 2026 by the author. Published by *Naturalis Scientias*. This is an open access article under the Creative Commons Attribution-NonCommercial 4.0 International (CC BY-NC 4.0) License. (https://creativecommons.org/licenses/by-nc/4.0/).

---

1. Introduction

Rubidium and cesium exhibit high chemical reactivity and excellent photoelectric properties; consequently, they are widely used in traditional sectors such as photoelectric conversion devices, optical crystals, optical glass, catalysts, specialty glass, biochemistry, and medicine. Owing to these outstanding physicochemical properties, they also serve indispensable roles in emerging high-tech industries and the defence sector. Currently, the application of rubidium in optical technologies, synthetic catalysis, and specialty glass and ceramics represents a leading frontier in the development of emerging industries (Sun, 2013; Sun et al., 2013; Wang et al., 2024; Wang et al., 2025).

Benefiting from diverse and favorable geological settings, mainland China possesses abundant and widely distributed rubidium resources, encompassing both solid-state deposits and various liquid (hot spring) brine-type deposits (Sun, 2013; Sun et al., 2013; Wang et al., 2024).

The rare metal rubidium is a key material for the development of strategic emerging industries under China's "13th Five-Year Plan" (Hou, 2023). Over the past two decades, there has been a surge in exploration and research regarding rare and critical metals—including rubidium—across mainland China, leading to breakthroughs in numerous areas.

Drawing on the latest research by Chinese scholars, this paper classifies the genetic types of rubidium deposits in mainland China, summarizes the geological characteristics of these various deposit types, and offers a preliminary discussion on their formation mechanisms.

2. Characteristics and current status of rubidium resources

Rubidium deposits in mainland China are primarily distributed across 12 provinces and autonomous regions—including Jiangxi, Xinjiang, Hunan, Sichuan, Yunnan, Tibet, Qinghai, Shaanxi, Henan, and Guangdong (Fig. 1)—and are predominantly of super-large and large scale (Sun et al., 2015; Sun et al., 2019; Gao et al., 2023).

Tectonically, rubidium mineralization in mainland China primarily occurs within rare-metal metallogenic belts such as the eastern segment of the Jiangnan Uplift, the Wugongshan–Northern Wuyishan belt, the central Nanling belt, the Central Zhejiang–Wuyishan belt, the Kangdian region, the Altay region, and the northern margin of the North China Craton. Granite-hosted and (granite-) pegmatite-hosted deposits constitute the main types of rubidium deposits in the country, though they are predominantly associated/paragenetic resources. The fundamental pattern of inherent scarcity regarding rubidium resources in mainland China has not yet undergone substantial change (Sun et al., 2019). In the first half of 2025, 38 new mineral deposit sites were discovered nationwide, representing a year-on-year increase of over 30% (Yi, 2025). Significant breakthroughs were achieved in the exploration for strategic/critical metals—including uranium, rubidium, gold, cobalt, and manganese—with the discovery of a number of large-scale and super-large deposits. Notably, the addition of 3.37 million tonnes of rubidium resources in Xinglong County,

Hebei Province—reaching a super-large scale—has further consolidated China's dominant global position in rubidium resources.

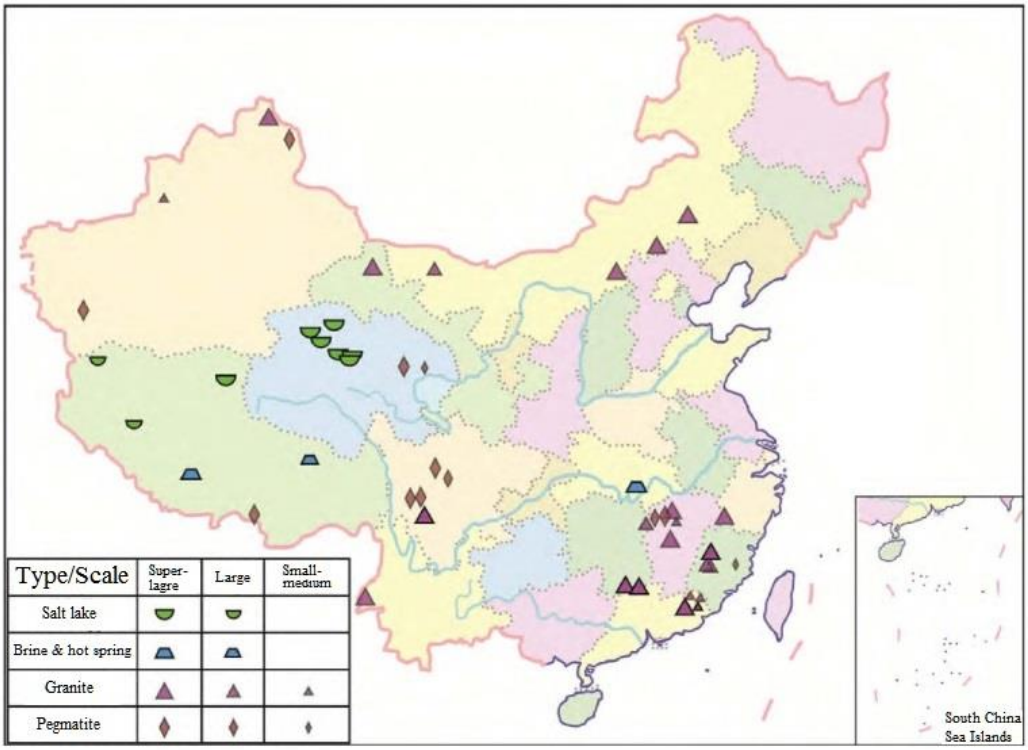


Figure 1. Distribution map of rubidium (and cesium) deposits in China (after Gao et al., 2023)

Although mainland China possesses abundant rubidium resources—a critical metal—almost all currently known deposits are granite-hosted associated resources characterized by low grades, difficult extraction, and processing challenges. High-grade, easily processed granite-pegmatite-hosted rubidium deposits—featuring ore minerals such as zinnwaldite, lepidolite, and pollucite—are extremely limited (Wu et al., 2021; Tang and Wu, 2024). The metallogenic ages of associated/paragenetic rubidium deposits in mainland China are concentrated within specific periods, and no independent rubidium deposits have yet been discovered (Sun et al., 2013).

Rubidium primarily occurs in pollucite, lepidolite, microcline, and roscoelite, with some occurrences in Nb-Ta-Mn minerals and biotite. It mainly substitutes for potassium via isomorphous replacement in minerals such as biotite, muscovite, and K-feldspar. Gangue minerals include quartz, K-feldspar, and mica (Sun, 2013; Xing, 2020).

Rubidium resources in mainland China consist primarily of solid hard-rock deposits, with reserves (as Rb_2O) totalling 1.16 million tonnes (Wang et al., 2024). While acid-based extraction from solid ores is currently the dominant method for industrial-scale production, solvent extraction and ion exchange hold immense promise for processing liquid-phase

rubidium resources. Wang et al. (2024) highlight the significant development potential of surface and subsurface brine-type rubidium resources; they recommend intensifying resource surveys and exploration, advancing technologies for the comprehensive beneficiation of low-grade solid and liquid ores, and expanding the application scope and functional capabilities of rubidium products.

Meanwhile, Sun et al. (2013) suggest that China prioritize the exploration and development of high-grade mica-hosted rubidium deposits, while also focusing on rubidium recovery from existing mine tailings and strengthening research into beneficiation processes and comprehensive utilization.

3. Genetic types and their geology

There is currently a broad consensus within the industry in mainland China that rubidium mineralization within the country can be classified into several types—including granite-hosted, (granitic) pegmatite-hosted, greisen-hosted, magmatic-hydrothermal, salt lake, subsurface brine, weathered granite crust, and placer types—with hard-rock mineralization (specifically granite and granitic pegmatite types) predominating; the Yanshanian period represents the most significant era of mineralization (Shen et al., 2003; Hou, 2023). While different hard-rock rubidium mineralization types exhibit distinct prospecting indicators, most are closely associated with albitization, amazonitization, and micatization, and are rich in volatile-bearing minerals such as fluorite and tourmaline. These endogenic rubidium deposits are closely linked to Yanshanian granites and often display horizontal and vertical zonation (Shen et al., 2003).

Based on publicly available data regarding rubidium deposits in mainland China, this paper reclassifies their genetic types, paying particular attention to specific details. For instance, mineralization previously termed "greisen-type" is, in reality, altered granite and is thus fully subsumed into the broad category of granite-hosted deposits. As there is no fundamental difference between salt lake and subsurface brine types, they are collectively categorized as "brine-hosted" deposits, further subdivided into surface water body and deep brine subtypes; additionally, an oil-and-gas-associated subtype has been added, alongside a Quaternary hot spring type, which ranks at the same hierarchical level as the brine-hosted category. The hard-rock category has been expanded to include skarn, porphyry, and volcanic rock types, while the solid-state category now includes the weathered granite crust type (Table 1); these are briefly described below.

3.1 Endogenic rubidium deposit

This type of rubidium mineralization is closely associated with tectono-magmatic activity; indeed, many deposits of rare and dispersed metals in mainland China are closely linked to tectono-magmatic activity within orogenic belts (Fig. 1 and Table 1).

Table 1. Genetic types and geology of rubidium deposits in Mainland China

Type		Geology	Origin/representative deposit	Data source
Endogenous	Pegmatite (broad sense)	In all pegmatite dikes—including microcline pegmatites, muscovite granite pegmatites, and muscovite-albite-spodumene pegmatites; Rb primarily occurs in minerals such as microcline and muscovite.	The Jiajika polymetallic deposit in Sichuan; numerous pegmatite dikes across the Qinghai-Tibet Plateau, Xinjiang, Sichuan, and the Eastern Qinling Mountains; the Shihuiyao deposit in Inner Mongolia, etc.	Du, 1983; hao, 1987; Wang, 2009; Liu et al., 2010; Sun, 2013; Duan et al., 2016; Xu et al., 2016; Sun et al., 2017; Yang, 2017; Guo, 2019; Yu et al., 2019; Zhang, 2019; Li, 2020; Wang et al., 2020; Xue et al., 2020; Kong et al., 2021; Chen et al., 2022; Fan et al., 2022; Liu, 2023; Xie et al., 2023; Chen et al., 2024; Fang et al., 2024; Li et al., 2024; Qin et al., 2024; Wang et al., 2024; Wen et al., 2024; Ban et al., 2025; Du et al., 2025; Li et al., 2025; Liang et al., 2025; Wang et al., 2025; Xie et al., 2025; Zhu et al., 2025; Cheng et al., 2026; Sha, 2026; Yin, 2026c, 2026d and 2026e; Yuan, 2026
	Magmatic-hydrothermal	These include hydrothermal vein types—such as quartz veins, often coexist and/or are associated with mineralization types such as quartz veins, explosive breccias, porphyry deposits, and skarns.	Inner Mongolia's Vilasto deposit, Xilinhot's Shihuiyao, northern Guangdong, the Qinghai-Tibet Plateau, and Sichuan's Jiajika, etc.	
	Cryptovolcanic breccia	The formation of crypto-explosive breccias is closely linked to the intense accumulation and explosive release of magmatic-hydrothermal fluids; consequently, some classify them as belonging to the magmatic-hydrothermal category.	The Weilasituo deposit in Inner Mongolia, among others.	
	Granite (broad sense)	Granite-hosted Rb deposits—which represent the most economically valuable Rb resource—encompass a wide variety of types, including albitized and K-feldspathized granites, granite-hosted disseminated deposits, greisenized granites, metamorphosed granites, autometamorphosed granites, alkaline or alkali-feldspar granites, monzogranites, fine-medium grained monzonites, fine-grained muscovite granites, coarse-grained to pegmatitic granites, microgranites, fine-grained muscovite-spodumene granites, and even (muscovite) albitites; these deposits are predominantly found within Mesozoic folded orogenic belts.	The Qinghai-Tibet Plateau and surrounding areas, Tengchong and Gejiu in Yunnan, Inner Mongolia, Zhengchong in Hunan, Tongcheng in Hubei, northern Guangdong, Xianglushan in Guangxi, and Jiajika in Sichuan, among others.	
	Alkaline igneous rock	Ferro-sodic alkaline basic rocks, ferro-potassic trachyte, ferriferous alkaline diabase and gabbro, alkaline (ferriferous) picrite, tephrite, alkaline syenite, and albitite, etc.	Areas such as Dongchuan in eastern Yunnan, as well as Henan and Shaanxi.	
	Porphyry	These include quartz porphyry and granite porphyry; Rb mineralization occurs primarily within quartz porphyry dikes and their contact zones with the surrounding rock, with Rb substituting for other elements within muscovite or biotite, and the mineralization is closely associated with silicification and sericitization.	Rb deposits such as those in Jianning (Fujian), Zhengchong (Hunan), and Ningguo (Anhui).	
	Skarn	Skarn-type Rb mineralization associated with syn-collisional granites frequently co-occurs or is associated with various other metals, forming a concentration zone of ferrous, non-ferrous, and rare (or even rare-earth) metal mineralization.	Polymetallic mineralization in Diantan, Tengchong, Yunnan, etc.	
	Volcanic	Occurs in rhyolite porphyry.	Siziwang Banner, Inner Mongolia.	
Superposition of endogenous and exogenous factors	Hot spring	It is commonly found along the Yarlung Tsangpo Suture Zone on the Qinghai-Tibet Plateau and in surrounding regions, such as southern Tibet, Sichuan, and Yunnan.	It is commonly found on the Qinghai-Tibet Plateau and in surrounding areas such as Sichuan and Yunnan.	
	Brine	Including surface water subtypes such as salt lakes, as well as underground brine subtypes and oil and gas field subtypes.	It is commonly found on the Qinghai-Tibet Plateau and in surrounding areas such as Sichuan and Yunnan.	
	Coal	Various rare metals are present in many coalfields across mainland China.	They are found in the Northeast, Northwest, North China, Central-South, and Southwest regions, among others.	
Exogenous	Weathered granite crust and placer	The Dayangtian rubidium deposit in Tengchong, Yunnan, features a weathering-crust type rubidium deposit near the surface; the primary rubidium-bearing minerals include potassium feldspar, albite, and mica.	Tengchong, Yunnan, and other areas.	

3.1.1 Porphyry-type

These include rock types such as quartz porphyry and granite porphyry. For instance, in the rubidium deposit near Dongkeng Village, Jianning County, Fujian Province, the host rocks consist primarily of quartz porphyry, with subordinate amounts of cataclasite and granite porphyry. The average Rb_2O grade is approximately 0.13%, with associated tin; the delineated rubidium resource is currently classified as large-scale. The rubidium ore bodies occur mainly within quartz porphyry dikes and their contact zones with the country rock, and are strictly controlled by NE-trending faults (dipping northwest with steep attitudes) (Yang, 2017; Li, 2020). The country rocks comprise the Tianjingping Formation leptynite and Caledonian-age migmatite; mineralization is closely associated with silicification and sericitization. Within the ore, rubidium occurs via isomorphous substitution for K^+ in altered K-feldspar, muscovite, and biotite (Yang, 2017). The ore-forming materials originated from Caledonian basement rocks characterized by high background levels of Rb and Sn; these materials were mobilized, transported, and enriched within shallow fault

zones and porphyry contact zones by Late Yanshanian (approx. 140–100 Ma) magmatic-hydrothermal processes. The deposit is classified as a porphyry-contact metasomatic Rb-Sn deposit, closely linked to intermediate-acidic magmatism associated with the large-scale extensional tectonic setting of the Yanshanian period in South China.

The Zhengchong Rb-polymetallic deposit in Hunan Province, located in the central section of the Nanling Rb metallogenic belt, is a super-large, Rb-dominant rare-metal deposit associated with highly fractionated granite (Fig. 2). The ore bodies are hosted within a zinnwaldite-bearing porphyry body; phenocrysts include quartz, zinnwaldite, and topaz, with zinnwaldite serving as the primary Rb-bearing mineral (Liu, 2023). The micas in this porphyry are almost exclusively zinnwaldite, with muscovite being rare; the high F content in the zinnwaldite and relatively low F content in the topaz reflect characteristics of a magmatic origin. Monazite within the fine-grained greisenized porphyry exhibits a high average Th content of up to 7.0 wt.%, alongside Th/Ce, Y/LREE, Ca/Ce, and Si/Ce ratios indicative of a magmatic origin. The whole-rock Y/Ho ratio of the greisenized porphyry approximates that of chondrites (240.01), serving as a petrological marker for Rb-Li-Cs rare-metal exploration in the region. This porphyry likely underwent three superimposed stages of in-situ crystallization, leading to the extreme enrichment of incompatible elements and the eventual formation of an Rb-Li-Cs rare-metal deposit.

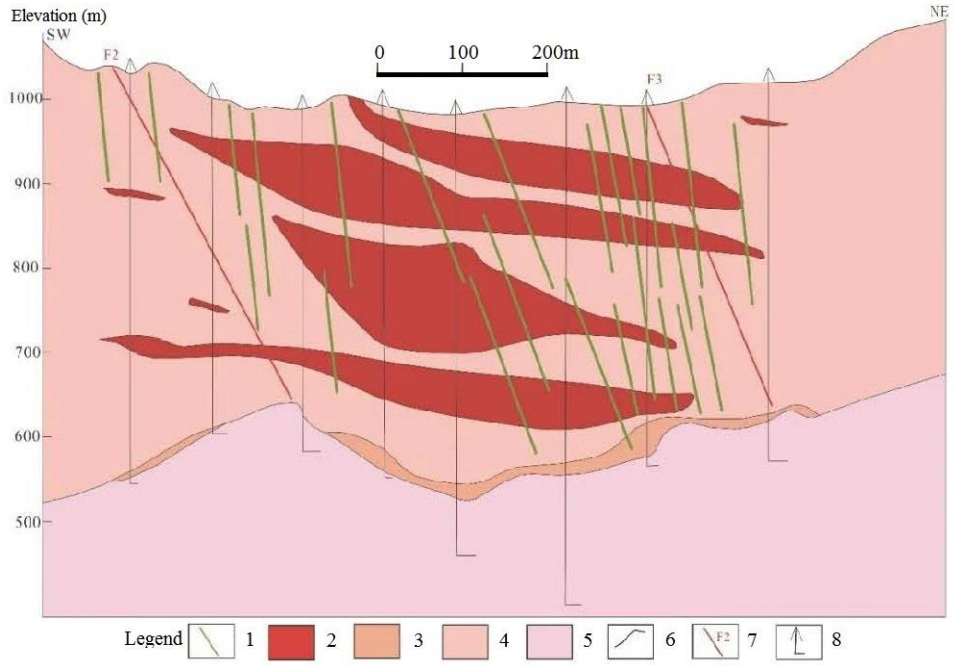


Figure 2. Section of the Zhengchong greece porphyry Rb polymetallic deposit in Hunan, China (average grade: Rb_2O 0.225%, Li_2O 0.557%, Cs_2O 0.012%. Quoted from Wen et al., 2024)

1-Quartz-vein type tungsten deposit; 2-Greisen-type lithium deposit; 3-Granite-type lithium deposit; 4-Porphyritic biotite granite; 5-Medium- to fine-grained alkali-feldspar granite; 6-Geological boundary; 7-Fault; 8-Drill hole

The Xiwukou rubidium deposit, located in the Jiangnan Uplift Belt, is the first critical metal deposit discovered in Ningguo, Anhui Province, in recent years; the associated magmatic rock is granite porphyry (Chen et al., 2022). Two types of rubidium ore bodies are present: Ore Body I occurs as a lens at the top of the granite porphyry body, with phengite content reaching 70% and a grade of 0.25%; Ore Body II occurs at the contact zone between the granite porphyry and the surrounding strata, with a grade of 0.21%. Both types of ore bodies share a mineral assemblage of phengite and quartz. Electron probe micro-analysis (EPMA) and laser ablation inductively coupled plasma mass spectrometry (LA-ICP-MS) studies on the ore-forming intrusion and the major minerals within the ore bodies reveal that the average Rb contents in plagioclase, K-feldspar, and biotite from the granite porphyry are 3.10×10^{-6}, 872×10^{-6}, and 1328×10^{-6}, respectively; while the average Rb contents in phengite from Ore Bodies I and II are 2544×10^{-6} and 2686×10^{-6}, respectively. Crystal-chemical calculations indicate that rubidium enters the phengite crystal lattice via $Rb^{+} \rightarrow K^{+}/Na^{+}$ substitution—existing in the form of isomorphous replacement. The ore-forming magma of the Xiwukou deposit is characterized by high background Rb values and fluorine content. Mineral crystallization enriched Rb in the residual magma; during the transition from the magmatic to the hydrothermal stage, the high F content caused the framework silicate structure of the original magmatic system to transform into a layered structure, thereby facilitating the crystallization of abundant Rb-rich phengite and ultimately leading to the formation of the rubidium ore bodies.

3.1.2 Magmatic-hydrothermal + explosive breccia type

The formation of crypto-explosive breccia is essentially driven by the intense accumulation and high-pressure explosive release of magmatic fluids (gases and liquids). Consequently, researchers classify crypto-explosive breccia-hosted rubidium mineralization within the broader category of magmatic-hydrothermal systems.

The Weilasituo deposit in Inner Mongolia hosts three types of ore bodies: alkali-feldspar granite-hosted Sn-Rb, crypto-explosive breccia-hosted Li-Rb, and quartz vein-hosted Sn. The crypto-explosive breccia-hosted ore body is situated between the other two types. Focusing on quartz crystals and their fluid inclusions within the crypto-explosive breccia ore, Wang et al. (2024) employed techniques such as quartz cathodoluminescence, microthermometry of fluid inclusions, laser Raman spectroscopy, and in-situ oxygen isotope analysis. Their findings indicate that the quartz crystals underwent three growth stages: Q1, Q2, and Q3. While fluid inclusion salinity remained similar between stages Q1 and Q2, homogenization temperatures decreased and quartz oxygen isotope values became lighter, signalling an increased influx of meteoric water. The Weilasituo crypto-explosive breccia-hosted ore resulted from crypto-explosive activity at the top of the intrusion; as depressurized magmatic-hydrothermal fluids ascended, they mixed to varying degrees with meteoric water, triggering the precipitation of Li-rich micas and the associated Li-Rb mineralization.

In essence, the Weilasituo crypto-explosive breccia-hosted ore represents a form of granite-related or magmatic-hydrothermal Rb-polymetallic mineralization, albeit one where fluid-gas interactions have altered the ore's texture and structure.

3.1.3 Skarn-type

The Diantan skarn belt in Tengchong is situated at the junction of the Lhasa Block and the Indian Plate; it represents a concentration zone of skarn-type Fe-Cu-Pb-Zn and rare-metal mineralization associated with Early Cretaceous syn-collisional granites. Research by Cheng et al. (2026) indicates that the rubidium (Rb) ore bodies within the Diantan skarn belt typically occur alongside iron ore bodies within the skarn bodies and are accompanied by polymetallic mineralization involving Cu, Pb, Zn, Sn, W, and Mo. Seventeen major Rb ore bodies occur as stratiform, lenticular, and/or vein-like bodies, reaching lengths of up to 808.0 m; individual drill-hole intercepts show thicknesses of 1.02–11.28 m and average Rb grades of 0.040%–0.113%. Both the iron and rubidium resources are classified as large-scale deposits. Electron probe micro-analysis (EPMA) data for phlogopite show contents of SiO_2 (40.91%–41.39%), MgO (26.42%–26.87%), Al_2O_3 (14.30%–14.65%), K_2O (10.11%–10.45%), Na_2O (0.17%–0.19%), FeO (2.03%–2.27%), and TiO_2 (0.06%–0.11%). In-situ trace element analysis reveals Rb contents of 2,485–2,641 ppm; Rb, Sn, Cs, Ba, Li, B, Pb, Zn, Ga, and Nd are relatively enriched, whereas Sc, V, Cr, Co, Ni, Cu, Sr, and Zr are relatively depleted. Rare earth element (REE) contents are extremely low (41.9–253.2 ppb). The rubidium is hosted within phlogopite and formed during the late stage of skarn evolution. The Tengchong-Diantan skarn-type Fe-polymetallic ore belt extends over 40 km from north to south and is approximately 20 km wide from east to west. Phlogopite is present in several skarn-type deposits within the belt—such as the Tongchangshan Pb-Zn deposit—indicating potential for rubidium exploration.

3.1.4 Granite type

Granite-hosted rubidium deposits are known by various, albeit closely related, terms—such as albitized granite, K-feldspar-altered granite, disseminated granite-hosted, metamorphosed granite, autometasomatic granite, and greisen types (Du, 1983)—as well as alkaline granite, monzogranite, and medium-to-fine-grained monzonite types.

Granite-hosted rubidium deposits represent the most economically valuable rubidium resource (Xie et al., 2023). As a vital resource base for national strategic minerals and critical metals, granite-hosted rubidium deposits in the Qinghai-Tibet Plateau are predominantly located within Mesozoic folded orogenic belts and associated with large-scale faulting; alteration processes—specifically albitization, greisenization, and amazonitization—are closely linked to mineralization. Numerous granite-hosted and pegmatite-hosted rubidium (or rubidium-polymetallic) deposits with large- to super-large-scale resource potential have been identified in the Qinghai-Tibet Plateau (Xie et al., 2023).

In Hunan, granite-hosted mineralization involving lithium, rubidium, niobium, tantalum, and other rare metals is concentrated in the Early Yanshanian (Jurassic) and Late Yanshanian (Late Cretaceous) periods; for instance, the monazite U-Pb age of the Zhengchong Li-Rb-Cs deposit in Hunan is 148–150 Ma (Wen et al., 2024), while the mineralization age of the Shihuiyao granite-hosted Rb-polymetallic deposit in Inner Mongolia is 144.7 Ma (determined via $^{40}Ar/^{39}Ar$ geochronology; Sun, 2013).

Granite-hosted rubidium mineralization occurs in association not only with other rare and non-ferrous metals but sometimes with non-metallic mineral resources as well. For

instance, the recently discovered super-large rubidium deposit in Tongcheng, Hubei Province, is hosted within greisenized granite used for ceramics; this deposit is situated in the greisenized granite along the northeastern margin of the Mufushan granite batholith (Xue et al., 2020).

The primary rubidium-bearing minerals at the Dayangtian rubidium deposit in Tengchong, Yunnan Province, are K-feldspar, albite, and mica (Du et al., 2025). The ore-forming materials originated from acidic magma enriched in rare and non-ferrous metals; post-magmatic fluids, formed as the magma ascended along fault structures, facilitated the further enrichment of rubidium. The sedimentary wall rocks—comprising the Gaoligongshan Group and Carboniferous clastic rocks—served as an effective cap rock, successfully retaining the rubidium-bearing fluids and ultimately leading to the formation of the granite-hosted rubidium deposit.

The Shihuiyao Rb-Nb-Ta deposit in Xilinhot, Inner Mongolia, is a large rare-metal polymetallic deposit associated with alkaline granite. The principal niobium and tantalum minerals in the ore include manganocolumbite, columbite-tantalite, manganocolumbite-tantalite, manganotantalite-cassiterite, and microlite (Duan et al., 2016). This deposit resulted from the combined effects of early-stage magmatic crystallization and late-stage hydrothermal metasomatism, with the latter representing the primary mineralization stage for niobium, tantalum, and rubidium. Mineralization is closely linked to albitization and greisenization; the ore bodies are hosted within altered granite and are strictly controlled by northeast-trending structures. Albitized and greisenized granites serve as direct indicators for prospecting these rare metals.

Granite-hosted rubidium polymetallic mineralization rarely occurs in isolation; it is frequently associated with other rare metals, rare earth elements, base metals, ferrous metals, and even non-metallic minerals. Such mineralization often exhibits distinct zoning patterns. A prime example is the Liangyuan Nb-Ta-Rb-W polymetallic deposit, situated at the intersection of the east-west trending Nanling tectonic-magmatic belt and the northeast-trending Wuyishan tectonic belt. This deposit represents one of the most significant breakthroughs in recent years regarding the exploration and assessment of quartz-vein type tungsten deposits, greisen-type Nb-Ta-Rb-W deposits, and granite-hosted Nb-Ta-Rb polymetallic deposits in northern Guangdong Province (Fan et al., 2022). Four new Nb-Ta-Rb-W ore bodies have been discovered, with resources comprising 3,425.72 tonnes of Nb_2O_5 (average grade 0.0108%), 1,428.99 tonnes of Ta_2O_5 (average grade 0.00449%), 8,205.14 tonnes of WO_3 (average grade 0.25%), and 61,398.73 tonnes of associated Rb_2O (average grade 0.0987%). The Liangyuan deposit features quartz-vein type tungsten polymetallic ore bodies and greisen-type Nb-Ta-Rb-W ore bodies in its shallower sections, while granite-hosted Nb-Ta-Rb ore bodies occur at greater depths. Zircon SHRIMP U-Pb dating indicates that the formation age of the greisen ranges from 163.6 to 159.2 Ma, while the weighted mean $^{206}Pb/^{238}U$ age of zircons from the biotite granite is 163.0 ± 1.6 Ma. Muscovite ^{40}Ar-^{39}Ar isochron dating yields mineralization ages of 166.4 ± 1.1 Ma for the greisen-type ore bodies and 168.7 ± 1.2 Ma for the muscovite granite-hosted ore bodies. The Liangyuan Nb-Ta-Rb-W deposit formed during the Middle to Late Jurassic; it is a product of the onset of large-scale Mesozoic granitic magmatism and associated Nb-Ta-Rb polymetallic mineralization in eastern South China, as well as a product of extreme granitic magma fractionation. The timing of rock formation and mineralization is essentially

synchronous. The deposit features quartz vein-type tungsten ore and greisen-type W-Sn-Nb-Ta-Rb mineralization in the shallow zones; greisen-type W-Nb-Ta-Rb ore bodies at the contact zone of the intrusion; and highly fractionated granite-hosted Nb-Ta-Rb ore bodies at depth.

Li et al. (2024) investigated the Xianglushan Rb deposit in Guangxi using techniques such as chemical analysis, optical microscopy, TIMA, and LA-ICP-MS. They identified muscovite, K-feldspar, and plagioclase as the Rb-bearing minerals in the ore, with Rb content decreasing in the order of muscovite > K-feldspar > plagioclase. Although K-feldspar is the primary host mineral for Rb, the distribution of Rb within it is heterogeneous. In both monzogranite and medium-to-fine-grained monzonite, K-feldspar accounts for over 80% of the total Rb, indicating that the Xianglushan Rb deposit is a feldspar-hosted Rb resource.

As one of the world's largest hard-rock rare-metal deposits, the Jiajika rare-polymetallic ore field in western Sichuan is a site of significant importance in mainland China. The Jiajika ore field is composed of (Li-mineralized) fine-grained muscovite granite, coarse-grained/pegmatitic granite, and fine-grained granite pods or lenses, spatially superimposed or intersected by quartz pods or veins (Sha, 2026). Lithium is enriched in spodumene; rubidium is hosted in microcline and muscovite; niobium and tantalum are hosted in columbite-tantalite group minerals and muscovite; beryllium is enriched in beryl; and tin is primarily enriched in cassiterite. Sha (2026) classified the mineralization types in the Jiajika ore field into Li, Rb, Nb-Ta, Be, and Sn mineralization types. Based on correlation and cluster analyses, the elemental assemblages are categorized into three groups: Li, Rb, and Nb-Ta-Be-Sn. Rb-mineralized granites exhibit high total alkali content and are characterized by high Al, K, and Na; Nb-Ta-Be-mineralized granites belong to the calc-alkaline series and are characterized by low K and high Na; while Li-mineralized granites are enriched in Si and depleted in Na and K. Rb-mineralized granites show a positive K anomaly and a distinct negative Nb anomaly. In contrast, Nb-Ta-Be-mineralized granites exhibit a negative K anomaly. Li-mineralized granites share significant similarities with Nb-Ta-Be-mineralized granites, with the primary difference being the relative depletion of K in the Li-mineralized granites. Rubidium-mineralized granites exhibit notably low rare-earth element (REE) contents and lack significant negative Eu anomalies; compared to other rock types, their REE distribution patterns show the shallowest slopes and the lowest degrees of fractionation. The distinction between Nb-Ta-Be-mineralized granites and Li-mineralized granites lies in the fact that the latter possess higher total REE contents; relative to the Jiajika granite body and Rb-mineralized granites, both types exhibit relatively low heavy REE contents and pronounced negative Eu anomalies.

Yuan (2026) classified the igneous rocks in the Jiajika mining area into seven types: (muscovite) microcline pegmatite, muscovite granite pegmatite, muscovite-albite-spodumene pegmatite, fine-grained (inequigranular) muscovite-spodumene granite, fine-grained (inequigranular) muscovite granite with industrial-grade Be mineralization, fine-grained (inequigranular) muscovite granite with industrial-grade Nb-Ta mineralization, and fine-grained (inequigranular) muscovite granite. It was noted that lepidolite is virtually absent from the granitic dikes in the Jiajika area and that rock-type zoning is indistinct. The granitic rocks of the Jiajika area belong to the calc-alkaline series. Li-mineralized granitic dikes are characterized by low Na contents; Be- or Nb-Ta-mineralized dikes by high Na;

and Rb-mineralized dikes by high K and moderate Na. The K/Rb ratio decreases as the degree of mineralization increases. Rare-metal mineralization in the Jiajika area primarily involves Li, Be, Rb, Nb, and Ta. The Jiajika deposit is a granite-dike-hosted rare-metal deposit associated with a Triassic granite dome.

The Shihuiyao Rb-polymetallic deposit in Inner Mongolia, discovered in 2010, is a super-large rare-metal deposit where rubidium is the primary commodity. Muscovite ^{40}Ar-^{39}Ar dating yielded a weighted mean age of 144.7 ± 1.1 Ma and an isochron age of 143.3 ± 1.4 Ma for muscovite from greisenized granite; for flaky muscovite from pegmatite dikes, the weighted mean age was 146.4 ± 1.0 Ma and the isochron age was 143.9 ± 1.5 Ma (Sun et al., 2015). The deposit formed during the Late Yanshanian period. The mining area is characterized by intense folding, well-developed faulting, and frequent, widespread magmatic activity. Large-scale amazonite-bearing granite, greisenized granite, and some granitic pegmatites are distributed within the area, with albite alteration developed in the rocks.

In Nading Village, Cona County, Shannan Prefecture, Tibet, metamorphic and intrusive rocks are well-developed; mineral resources consist primarily of rubidium, beryllium, and lithium, with aquamarine as a secondary commodity. Rare-metal mineralization occurs within muscovite-albite rock and monzogranite (or monzogranitic pegmatite) bodies. Rubidium mineralization is ubiquitous across all granitic rock types in the area; the estimated rubidium metal resource (categories 3341) is 120.4634 million tonnes, classifying it as a super-large deposit (Wang, 2009).

Wang et al. (2025) predicted that potential resources of 780,000 tonnes of lithium and 260,000 tonnes of rubidium could be discovered within the greyish-white, fine-grained monzogranite of the Yangshan area in Gejiu, Yunnan Province.

3.1.5 Pegmatite type

In a broad sense, pegmatite-type rubidium mineralization encompasses granitic pegmatites.

The East Qinling region is a significant area for the distribution of granitic pegmatites and the metallogenesis of rare metals in China; it features a wide variety of granitic pegmatite dikes, forming four distinct zones of concentrated dike swarms. Research by Xu et al. (2016) on the Ziyugou granitic pegmatite-hosted rubidium deposit in Danfeng, Shaanxi, indicates that the Variscan-age, rubidium-bearing granitic pegmatite dikes in the area are large in scale and laterally extensive, exhibiting uniform rubidium mineralization and high Rb_2O content. The Kuanping intrusive body serves as the parent rock for these dikes, with rubidium primarily hosted in microcline and muscovite.

The Tuanbaoshan rubidium deposit is located on the eastern shore of Qinghai Lake in Qinghai Province. Hosted within granitic pegmatite dikes cutting the Paleoproterozoic Huangyuan Group (Pt_1H), it is a large-scale feldspar-hosted rubidium deposit with associated rare metals such as niobium and tantalum (Liu et al., 2010). The deposit formed during the Caledonian period when highly evolved, volatile-rich pegmatitic magmatic-hydrothermal fluids—derived from a deep-seated magma chamber—intruded into ancient strata under the influence of NW-trending transpressional tectonic stress; slow

crystallization subsequently produced bead-like ore bodies. The pegmatite dikes in this deposit occur in large-scale clusters and belts.

The Changzheng-Yalakan granitic pegmatite-hosted rubidium deposit in Daofu County, Sichuan, is controlled by the interplay of magmatism, doming structures, and metamorphism. Late Indosinian to Yanshanian granitic pegmatites constitute the primary ore-bearing bodies, with an average Rb_2O content of 0.13% and a maximum of 0.64% (Qin et al., 2024). The Eastern Tibet region, a key component of the Sanjiang tectonic belt, is a major metallogenic zone for non-ferrous metals (Cu, Pb, Zn) and rare metals (Y, Nb, Ta, Os, Ir, Pt, W, Sn) (Yu et al., 2019). Within this region, the Jianong-Gexiong Nb-Ta-Rb rare-metal enrichment zone is a favorable area for prospecting for pegmatite-type Nb-Ta deposits, high-temperature hydrothermal Rb deposits, and medium-to-low-temperature hydrothermal Pb-Zn deposits.

3.1.6 Alkaline igneous rock type

Alkaline igneous magmas exert a unique control on the mineralization of rare-earth, rare, precious, and non-ferrous metals (including rubidium). Through large-scale tectono-lithofacies mapping of the Dongchuan Fe-Cu-Au ore cluster (a Proterozoic continental rift basin) and the Gejiu Sn-Cu-W-Cs-Rb polymetallic ore cluster (a Triassic back-arc rift basin), Fang et al. (2024) analyzed the volcanic-intrusive sequences, rock assemblages, rift basin evolution, and magmatic-superimposed intrusive structural systems associated with alkaline magmatism. Their study revealed the intrinsic relationships between these features and the superimposed mineralization of Eastern Yunnan-style iron oxide-copper-gold (IOCG) deposits, Cu-Co-rutile-REE deposits, and Sn-Cu-W-Cs-Rb polymetallic deposits. Key findings include: In the Dongchuan Fe-Cu-Au ore cluster, Neoarchean alkaline rocks are dominated by calcitite-albite rocks (2,520 ± 14 Ma) and alkaline ferriferous picrites (2,529 ± 77 Ma). A distinct geological unit (mapped independently as 2.50–1.80 Ga) was formed through the structural overprinting of Mesoproterozoic volcanic-magmatic activity onto the paleokarst weathered crust at the top of the Neoarchean-Paleoproterozoic Xiaoliukou Formation (>2.50 Ga); these units represent new target horizons for Cu-Co-rutile-REE exploration. Rock assemblages—including ferro-sodic alkaline basic rocks, ferro-potassic trachytes, and ferriferous alkaline diabase-gabbros within Member 1 of the Mesoproterozoic Yinmin Formation—formed during the volcanic fault-depression basin-forming stage of the Yinmin period. Members 2 and 3 of the Yinmin Formation serve as the host horizons for Xikuangshan-style Fe-Cu deposits, while the ferro-potassic trachyte in the footwall of the Fe-Cu ore layer acts as the host horizon for monazite-type REE mineralization. During the Grenville orogeny, alkaline mafic intrusive rocks—including alkaline Fe-Ti gabbro (1,097–1,047 Ma), alkaline Fe-Ti diorite, and alkaline monzonite porphyry—gave rise to the Baixila deep-seated IOCG deposit and rutile mineralization. Within the Triassic back-arc rift basin of Gejiu, initial enrichment of Sn, Cu, Zn, Li, Rb, and Cs occurred in Triassic alkaline picrites and tephrites; subsequent Late Cretaceous leucogranite-related superimposed mineralization formed phlogopite-skarn type Sn-Cu-W-Cs-Rb deposits. The superposition of later ore-metal-rich alkaline intrusions onto the initially metal-enriched early alkaline rocks within the rift basin likely constitutes the mechanism behind this extraordinary metal enrichment. In the Dongchuan area, within the structural setting of superimposed magmatic intrusions, magmatic-hydrothermal breccia

pipes played a significant role in controlling the superimposed enrichment and mineralization of Cu, Co, rutile, and rare earth elements. In the Gejiu area, the intrusion of leucogranites into alkaline picrites and tephrites exerted significant control over the superimposed enrichment and mineralization of phlogopite-skarn type Sn-Cu-W-Co-Cs-Rb deposits.

The Shimen rubidium deposit in Songxian County, Henan Province, is hosted within an Indosinian alkaline syenite body, which is composed primarily of K-feldspar (Li et al., 2015). Indosinian magmatism provided an abundant source of material for the formation of rare-metal and rare-earth element deposits—including rubidium—in the region; subsequent tectono-magmatic hydrothermal activity led to the partial mobilization and enrichment of rubidium within the intrusive body, resulting in the formation of the Shimen rubidium deposit.

3.1.7 Volcanic rock type

The Abuda'ertai rubidium and rare metal deposit is a newly discovered volcanic-hosted rare polymetallic deposit in Siziwang Banner, Inner Mongolia. The ore bodies are primarily hosted within the continental acidic volcanic rocks of the Upper Jurassic Baiyingaolao Formation (Liang et al., 2025), and their spatial distribution coincides with that of the rhyolitic porphyry of the same formation. Rubidium content is closely correlated with the intensity of albitization and kaolinization in the host rocks, with rubidium mineralization occurring throughout the rhyolitic porphyry. This area is one of the few rubidium exploration bases in Inner Mongolia with promising prospecting potential. Based on an analysis of the regional and local geological settings, deposit characteristics, ore fabric, and major, trace, and rare-earth element compositions, it is inferred that the formation of the deposit is closely linked to the volcanic rocks.

3.2 Endogenic-exogenic superimposed rubidium deposit

3.2.1 Quaternary hot-spring type

Quaternary hot-spring-type rubidium-cesium mineralization is commonly found along the Yarlung Zangbo Suture Zone on the Tibetan Plateau and in surrounding regions, such as southern Tibet and parts of Sichuan and Yunnan.

Active hot springs in the Tengchong area of Yunnan generally contain rare metals (e.g., Li, Be, Rb, and Cs) and trace elements (e.g., W, Sb, Tl, and Mo), with the enrichment of Li, Rb, Cs, and W being particularly notable. The average concentrations of Li, Rb, Cs, and W in the hot springs are 2,895.1 μg/L, 839.8 μg/L, 417.9 μg/L, and 61.74 μg/L, respectively (Guo, 2019). Rare metal concentrations increase correspondingly with higher spring water temperatures. Helium isotope data indicate a supply of mantle-derived material to the hot springs, and rare metal concentrations rise significantly as the proportion of mantle-derived components increases.

3.2.2 Brine-type

Similar to and often co-occurring with brine-type cesium deposits, brine-type rubidium deposits fall into three categories: surface water subtypes (such as various salt lakes and landlocked seas), underground brine subtypes, and oil/gas field subtypes (Table 1). They are primarily found in the Qinghai-Tibet Plateau and surrounding regions, including Sichuan, Yunnan, and Xinjiang.

Zhao (1987) utilized a natural ion exchanger from a specific location in China to directly adsorb K+, Rb+, and Cs+ from gas field water, while using local natural brine as the desorbent. The process is characterized by the use of natural ion exchangers as adsorbents and high-concentration natural brines as desorbents. It ingeniously combines barium removal from mirabilite with sulfate removal using barium chloride; this approach reduces potassium chloride production costs, prevents barium contamination of the table salt product, enhances the adsorption capacity of the natural ion exchanger, and inhibits calcium sulfate scaling in evaporation tanks. The process employs cold adsorption and hot washing, a single-stage adsorption and washing cycle, and cooling crystallization. Experimental results showed a barium removal rate of 99.81%, a total recovery rate of 77.15%, an 86.48% adsorption rate of K^+ by the natural ion exchanger, and a total potassium recovery rate of 72.10%. The barium sulfate met national Grade II standards, the potassium chloride met national Grade I standards, and the table salt met the Grade I standard for well salt; additionally, a byproduct solution containing 0.95 g/L of Rb and 3.4 g/L of Cs was obtained for the subsequent extraction of rubidium and cesium metals. Production costs were approximately 400 RMB per tonne for potassium chloride, 400 RMB per tonne for barium sulfate, and 80 RMB per tonne for table salt.

3.2.3 Coal type

An increasing number of studies indicate that numerous coal mines in mainland China contain various rare metals, including gallium, germanium, and cesium (Yin, 2026c, 2026d, and 2026e).

Currently, the primary raw materials for the industrial production of rubidium and cesium are solid ores such as pollucite and lepidolite; however, the extraction processes involved are complex and costly. China possesses vast coal reserves, amounting to trillions of tonnes. Because coal seams formed in unique geochemical environments, certain valuable trace elements became enriched within them. The concentrations of rubidium and cesium in some Chinese coal mines are remarkably high—six and twelve times the global average for coal mines, respectively. Clearly, rare metals like rubidium and cesium associated with coal deposits represent a potential resource that could serve as a source for these elements. Consequently, extracting rare metals such as rubidium and cesium from coal mines is of great significance for the comprehensive utilization of coal resources and the sustainable development of the coal industry.

In 2017, Sun et al. filed a patent for a method and process to separate and extract rubidium and cesium from coal. Once this technology is implemented on a large scale, it holds the potential to extract rare metals like rubidium from numerous coal mines, thereby transforming the global supply-demand landscape for rubidium resources.

3.3 Exogenic rubidium deposit

3.3.1 Weathered granite crust type and placer type

Such secondary rubidium deposits occur at the tops of and in the areas surrounding endogenous rubidium deposits, such as the aforementioned granite-hosted types. The near-surface and surrounding areas of the Dayangtian rubidium deposit in Tengchong, Yunnan, host weathered-crust and placer-type rubidium deposits (Du et al., 2025), where the primary rubidium-bearing minerals include K-feldspar, albite, and mica.

4. Ore control

4.1 Hard-rock type

Traditional ore-controlling factors for endogenic metal deposits—such as tectonics and magmatism—remain fundamental to the mineralization of rare metals, including rubidium (Yin et al., 2025). For instance, the northern margin of the Qaidam Basin in Qinghai—situated at the junction of the Paleo-Asian and Tethyan tectonic domains and characterized by a polycyclic arc-basin orogenic system—possesses favorable geological conditions for rare metal and rare earth element (REE) mineralization. Significant progress in critical metal exploration has been made in the region in recent years, leading to the discovery of numerous pegmatite-hosted Li-Be-Rb polymetallic deposits and occurrences; representative examples include the Shinaihai Nb-Ta-Rb deposit, the Amunege Rb-Nb-Ta deposit, and the Xiaridawu Nb-Ta-Rb deposit. The northern margin of the Qaidam Basin has emerged as a new, important metallogenic belt for rare metals and REEs in the northern Tibetan Plateau, demonstrating promising exploration potential for deposits associated with pegmatites and alkali-feldspar granites—specifically those containing Li, Be, Nb, Ta, Rb, La, and Ce (Kong et al., 2021). Given that the role of tectono-magmatic activity in controlling metal mineralization has been extensively discussed in existing literature (Yin et al., 2025), this paper will not reiterate those points. Instead, the discussion regarding the ore-controlling factors for rare metal mineralization (including rubidium) will focus on the specific conditions outlined below.

4.1.1 Magmatic fractional crystallization and hydrothermal metasomatism

Magmatic fractional crystallization and hydrothermal metasomatism are key factors controlling rubidium mineralization in granite, pegmatite, and skarn deposits.

Through major and trace element analyses of muscovite, K-feldspar, and plagioclase from Rb-bearing monzogranite, leucogranite, and greisen in the Xianglushan Rb mining area (northeastern Guangxi), Li et al. (2025) found that Rb concentrations in muscovite (3,826–9,100 ppm) were significantly higher than those in K-feldspar (2,423–2,770 ppm) and plagioclase (0.61–57.80 ppm); furthermore, Rb contents in all three minerals showed a positive correlation with the concentrations of volatile elements such as Li, B, and F. Rubidium primarily enters the crystal lattices of minerals like muscovite by substituting for K and Na ions via isomorphous replacement. Among the various types of Rb-bearing rocks,

greisen exhibited the highest Rb_2O content (averaging 0.1932%). Comprehensive research indicates that magmatic-hydrothermal metasomatism involving volatiles such as F is the dominant mechanism governing the partitioning and enrichment of rubidium in highly fractionated granitic rocks. The Xianglushan Rb deposit is the product of the combined effects of magmatic fractional crystallization and hydrothermal metasomatism.

4.1.2 Degree of magmatic differentiation

Hard-rock rubidium deposits in mainland China—particularly endogenic ones—are invariably closely associated with tectono-magmatic activity. Regarding the control of magmatism over endogenic rubidium mineralization, numerous scholars studying such deposits across various regions of mainland China have consistently identified highly fractionated granite bodies as a common characteristic associated with rubidium and related metal mineralization.

Wu et al. posit that the rare-metal mineralization associated with Yanshanian granites in the Nanling region is linked to the extensive fractional crystallization of granitic magmas (Wen et al., 2024). This crystallization differentiation manifests as the continuous, long-term segregation of crystal mushes and residual melts within the magma chamber. Coarse-grained porphyritic granites represent the cumulates (main body) formed during the early stages of crystallization, whereas fine-grained granites represent the residual, high-silica melts (complementary bodies). Whole-rock Zr/Hf and Nb/Ta ratios serve as indicators of the degree of granitic fractional crystallization. As the degree of magmatic fractionation increases, both whole-rock Zr/Hf and Nb/Ta ratios decrease significantly; notably, when the Nb/Ta ratio drops below 5, intense interaction occurs between the magma and fluids, marking a critical indicator of the granite's mineralization potential (Wen et al., 2024).

A study by Ban et al. (2025) on the Changchengling super-large Rb-Nb-Ta rare-polymetallic deposit in the central Nanling metallogenic belt reveals that the granite porphyry bodies in the area are characterized by high fractionation and whole-rock rubidium mineralization. Among them, the NW-trending Fengchui-Luodai concealed intrusion exhibits the highest Rb content (1,090–1,900 μg/g; average 1,410 μg/g), with mica serving as the primary Rb-enriched mineral. The distribution of the granite porphyry-type rubidium mineralization is controlled by the intersections of fault structures and zones where secondary structures are well-developed. The altered granite porphyry at the top of the concealed intrusive body is a favorable site for the occurrence of rubidium-rich ore bodies. The granite porphyry associated with rubidium-bearing rare-metal polymetallic mineralization formed during the Late Indosinian period. Sericitization at the top of the intrusion and secondary muscovitization at the contact zone between the intrusion and the country rock play a significant role in the enrichment of rubidium and other rare metals. The Changchengling deposit is hosted by granite porphyry, which serves as the parent rock for mineralization. To date, seven rubidium ore bodies have been delineated, trending northeast (NE), northwest (NW), and nearly north-south (SN).

Based on petrographic, whole-rock geochemical, and Nd-isotopic studies of the amazonite granite at Jiangjunshan in the Altay region of Xinjiang, Chen et al. (2024) determined that the amazonite granite is characterized by high SiO_2 (74.55%–77.93%), high K_2O (3.68%–4.37%), and high Al_2O_3 (A/CNK = 1.06–1.41), classifying it as a high-K calc-alkaline

peraluminous granite. The granite is enriched in Rb, Th, Ta, and Hf but strongly depleted in Ba and Sr; it exhibits a "seagull-shaped" rare earth element (REE) pattern, a strong negative Eu anomaly ($\delta Eu < 0.01$), and a tetrad effect ($TE_{1,3} = 0.92–1.21$). The amazonite granite displays extremely low whole-rock K/Rb (63–87), Nb/Ta (2.04–3.45), and Zr/Hf (8.43–9.96) ratios and contains fluorite and magmatic schorl. Geochemical and mineralogical characteristics indicate that the Jiangjunshan pluton underwent intense fractional crystallization and associated magmatic-hydrothermal processes. The amazonite granite formed during the Middle Permian and is cogenetic with the dominant two-mica alkali-feldspar granite. The high Rb content and A2-type granite affinity of the two-mica alkali-feldspar granite suggest it originated from the partial melting of biotite-rich igneous rocks. The petrogenesis and evolution of the Jiangjunshan amazonite granite indicate a high degree of evolution and significant fluid interaction, which played a crucial role in the enrichment of Rb within the granite. As a former accretionary wedge, the Altai region underwent continuous modification that effectively promoted the differentiation of newly formed crust and the creation of localized Rb-enriched source rocks, thereby providing the material basis for the formation of amazonite granite.

In summarizing the exploration models and targets for granite-hosted rare metal deposits (such as rubidium) in Hunan Province, Wen et al. (2024) concluded that the variations in Li, Rb, Nb, and Ta mineralization within the region are linked to the degree of high-level magmatic differentiation. Distinct stages of this differentiation process sequentially gave rise to Rb mineralization associated primarily with muscovite granite, Nb-Ta mineralization associated with muscovite (lepidolite) granite, and Li mineralization associated primarily with greisen (Jianfengling type). During the late stages of magmatic differentiation, Li-rich granites intruded into earlier granite bodies to form greisen-hosted Li-Rb deposits (Zhengchong type) or metasomatized the earlier granites to form altered granite-hosted Li deposits (Huishan type); meanwhile, post-magmatic hydrothermal fluids formed greisen-fluorite vein-type Li deposits (Jiepailing type) within structural fractures at the tops of the granite bodies. Five distinct types of rare metal deposits have been identified in Hunan Province: greisen (porphyry)-type Li-Rb-Cs deposits, muscovite (lepidolite) granite-hosted Li-Nb-Ta deposits, muscovite (two-mica) granite-hosted Rb deposits, altered greisen-type Li deposits, and greisen-fluorite vein-type Li deposits. The mineralization ages for these deposits cluster in two periods—the Jurassic (148–160 Ma) and the Late Cretaceous (86–89 Ma)—with the ore-forming materials derived primarily from magmas. The Zr/Hf and Nb/Ta ratios of the rocks serve as indicators of the rare metal mineralization potential of composite granite bodies.

4.1.3 Intensity of magma melt-fluid interaction and crustal contamination

Wu et al. propose that highly fractionated granites have generally undergone significant crustal contamination. Intense contamination by Al-rich crustal material can render the granite increasingly peraluminous; furthermore, such crustal material supplies abundant hydrous minerals, facilitating extensive magmatic evolution and enriching the magma in rare-metal ore-forming components. These characteristics likely serve as critical controls on the mineralization potential of highly fractionated granites. Taking Hunan Province as an example, highly fractionated granites exhibiting weak melt-fluid interaction show only moderate mineralization potential (Wen et al., 2024), whereas those with strong melt-fluid

interaction demonstrate high potential. Variations in Li, Rb, Nb, and Ta mineralization across Hunan are linked to the degree of magmatic fractionation; distinct stages of this evolution sequentially give rise to Rb mineralization (dominated by two-mica granite), Nb-Ta mineralization (dominated by muscovite granite), and Li mineralization (dominated by lepidolite granite and greisen), exemplified by the Jianfengling-type Li-Rb-Nb-Ta deposit (Wen et al., 2024). During the late stages of magmatic fractionation, Li-rich granites intruding into earlier granite bodies form greisen-type Li-Rb deposits (e.g., the Zhengchong-type Li-Rb-Cs deposit) or metasomatize the early granites to form altered-granite-type Li deposits (e.g., the Huishan-type Li deposit). Hydrothermal fluids from the final stages of magmatic evolution form greisen-fluorite vein-type Li deposits within structural fractures at the tops of granite bodies (e.g., the Jiepailing-type fluorite-Li deposit) or greisen-quartz vein-type W-Sn-Li deposits. Greisen (or greisen-porphyry) serves as a prospecting indicator for Li-Rb deposits, while granite Zr/Hf and Nb/Ta ratios act as petro-chemical markers for identifying rare-metal mineralization.

4.1.4 Oxygen fugacity and remelting of crust-derived materials

Highly fractionated granites are widely distributed across the Tibetan Plateau. A study by Xie et al. (2025) on the newly discovered super-large Gari'atong rubidium deposit in the central Lhasa terrane reveals that Rb mineralization primarily occurs within monzogranite and its host rocks; zircon U-Pb dating yields a weighted mean age of 20.0 ± 0.5 Ma (n=14, MSWD=1.8) for the ore-bearing monzogranite, indicating it is a product of Miocene magmatic emplacement. Rubidium occurs mainly via isomorphous substitution within muscovite and biotite. Geochemical characteristics of these micas indicate that the ore-forming magma originated from the remelting of crustal materials under low oxygen fugacity conditions; subsequent intense fractional crystallization generated a fluorine-rich magmatic-hydrothermal fluid, ultimately forming the large-scale rubidium deposit.

4.1.5 Alteration intensity

A study by Liang et al. (2025) on the Abudaertai Rb-bearing rare polymetallic volcanic-hosted deposit in Inner Mongolia revealed that the distribution of ore bodies coincides with that of the rhyolite porphyry of the Baiyingaolao Formation, and that rubidium content is closely correlated with the intensity of albitization and kaolinization in the host rocks.

The Chaharihada Rb rare-metal deposit in Inner Mongolia is hosted within a Late Triassic syenogranite body located at the northern end of a Hercynian-Indosinian composite batholith. Wang et al. (2020) proposed that mineralization is associated with hydrothermal alteration driven by highly evolved late-stage magmatic activity. The deposit exhibits intense metasomatic alteration and distinct zonation, progressing from a microclinization zone to an albitization zone and finally to a greisenization zone. The albitization zone and its transition zone with the greisenization zone constitute the primary zones of enrichment and mineralization for rubidium and other rare elements. Comparative analysis indicates that the Chaharihada Rb deposit bears strong similarities to the Duobaoshan Rb, Liujiahe Rb, and Qiyishan Rb-W-Sn deposits in terms of geotectonic setting, magmatic characteristics, host rocks, and ore assemblages; all belong to the category of magmatic-hydrothermal metasomatic alkaline to sub-alkaline granite-hosted deposits, characterized

by a favorable geological setting for mineralization and immense potential for rare-metal mineralization.

4.1.6 Fluxing elements and incompatible elements

According to Liu (2023), highly fractionated granites facilitate the formation of rare-metal deposits because they are enriched in incompatible elements (such as Li, Rb, Cs, Nb, and Ta) and fluxing elements (such as F, B, Cl, Li, P, and Na). Consequently, highly fractionated granites and pegmatites possess unique petrogenesis and significant economic potential.

The Beishan region, situated on the southern margin of the Central Asian Orogenic Belt, has undergone complex processes—including arc-continent accretion/collision and continental growth—along with multiple episodes of magmatism that resulted in the formation of Cu, Ni, and rare-metal deposits. Research by Zhang (2019) indicates a weighted mean LA-ICP-MS zircon U-Pb age of 427 ± 8 Ma for the amazonite-bearing granite. The evolutionary sequence of the granitic rocks in the study area progresses from biotite monzogranite to amazonite-bearing granite and finally to amazonite-bearing granitic pegmatite. Overall, SiO_2 content decreases along this sequence, while Al_2O_3 and (Na_2O + K_2O) contents increase; CaO content initially decreases and then increases; and MgO, TiO_2, Fe_2O_3, and P_2O_5 contents remain generally low. The rocks are Na-rich and K-poor, classifying them as peraluminous, high-K calc-alkaline granites. Overall, Sr and Ba contents are low but show wide variation, whereas Rb, Cs, and Pb contents are high; Rb, Nb, and Ta contents increase along the evolutionary trend; and the Nb/U, Y/Nb, and Rb/Sr ratios exhibit significant variation. Primitive mantle-normalized trace element spider diagrams reveal depletion in Ba, Sr, Nb, La, Ce, and Eu, and slight depletion in Y; strong enrichment in Cs, Rb, and Pb; moderate enrichment in Zr, Hf, U, and Th; and slight enrichment in Ta. The granites exhibit relatively low ΣLREE contents and high ΣHREE contents. On chondrite-normalized rare earth element (REE) patterns, the rocks exhibit a transition from LREE depletion to enrichment and from HREE enrichment to depletion, with (La/Yb)N ratios ranging from 0.13 to 4.21; the rock mass displays a strong negative Eu anomaly. The granite is classified as highly fractionated A2-type (PA-type) granite derived from a muscovite-rich source rock. Partial melting of the source rock generated a magma rich in fluorine, rubidium, and fluids. Magmatic evolution involved the fractionation of LREE-rich minerals (such as allanite and monazite) as well as plagioclase and K-feldspar. The Rb-bearing granite-pegmatite complex formed in a tectonic setting characterized by a transition from compression to extension following the closure of the South Tianshan Ocean basin. Muscovite served as the primary source of both the ore-forming element (Rb) and the ore-forming fluids. Melting of the muscovite-rich source rock produced a magma enriched in fluorine, rubidium, and fluids. Rb migrated as F-complexes until the late stages of magmatic evolution, when the complexes hydrolyzed; F^- then reacted with Ca^{2+} to form fluorite or was incorporated into minerals such as mica, while Rb entered feldspar to form mineralized amazonite-bearing granite.

The rare-metal metallogenic belt in western Yunnan, located in the southeastern Tibetan Plateau, is primarily distributed along the Nujiang and Lancangjiang fault zones. Its genetic types include granitic (including greisen), pegmatitic, skarn, tourmaline (sulfide)-quartz vein, phlogopite hydrothermal vein, weathered granite crust, coal-measure, and hot-spring

types. Notably, the granite- and pegmatite-hosted rare-metal deposits contain gemstone resources such as tourmaline and aquamarine. These deposits formed during six distinct periods: the Triassic (240–220 Ma), Early Cretaceous (124–120 Ma), Late Cretaceous (80–70 Ma), Paleocene–Eocene (65–50 Ma), Oligocene (33–30 Ma), and Miocene (25–12 Ma). These periods are associated, respectively, with the post-collisional setting following the closure of the Triassic Paleo-Tethys Ocean, the subduction of the Neo-Tethys Ocean, and the India-Eurasia collision followed by large-scale strike-slip shearing (Li et al., 2025). The Li-Be-Rb-Cs deposits in the region formed mainly during the Late Cretaceous, Paleocene–Eocene, and Miocene, with the Oligocene and Miocene mineralization events being closely linked to shear-related deformation and metamorphism. The deposits are characterized by F-enrichment, B-enrichment, or both, and are closely related to highly evolved granites from various periods. Indicator minerals such as cassiterite, tourmaline, and mica serve to trace the rare-metal mineralization processes and reveal variations in metallogenic element assemblages. Currently, exploration for Li-Rb-Cs is concentrated primarily in the Nujiang metallogenic belt. The Tengchong-Lianghe region is characterized primarily by granite-type and weathered granite-crust-type deposits (in the broad sense), whereas the Gaoligong region is dominated by pegmatite-type and phlogopite-hydrothermal-vein-type deposits (in the broad sense). Beryllium exploration is concentrated in the Gaoligong and Tengchong-Lianghe regions.

4.2 Hot spring and brine types

Studies indicate that rubidium mineralization associated with hot springs and brines in mainland China is controlled by several factors.

Zhu et al. (2025) analyzed stable isotopes (δD and $\delta^{18}O$) and elemental compositions of hot spring waters at Bukadaban Peak—a source area for salt lakes in the Qaidam Basin—and found that the hydrochemical types are primarily Na-Cl, Ca-HCO_3, and mixed Ca-Na-HCO_3. Concentrations of Li, Rb, and Cs in the hot springs vary by two to three orders of magnitude between high and low values, with levels increasing from the mountain slopes to the foothills. Fumaroles (steam vents) located on the slopes exhibit low Li, Rb, and Cs concentrations (averaging 10.6 μg/L, 19.9 μg/L, and 11.0 μg/L, respectively)—levels comparable to those in local shallow groundwater and river water, with Rb/Cs ratios >1. In contrast, hot springs at the foothills—characterized by lateral-to-vertical discharge and subsequent pooling—show high concentrations of Li, Rb, and Cs (averaging 69.1 mg/L, 11.5 mg/L, and 18.8 mg/L, respectively). The Rb and Cs distribution patterns in these waters resemble those of Tibetan hot springs (Rb/Cs <1), although the absolute concentrations of Li and Rb are higher. Hydrogen and oxygen isotope compositions indicate that the hot springs originate from a mixture of magmatic water, meteoric precipitation, and shallow circulating groundwater, with mixing occurring during the ascent of the thermal fluids. The concentrations of Li, Rb, and Cs are governed by multiple processes, including water-rock interactions involving deep-seated magmatic fluids, weathering and leaching by high-temperature shallow groundwater, and evaporative concentration at the surface. Their enrichment reflects a prolonged evolution involving the upwelling of magmatic fluids (and associated water-rock interactions), silicate weathering and leaching by shallow thermal waters, and subsequent surface accumulation, evaporation, and concentration.

4.2.1 Hot spring temperature

The content of rare metals in spring water increases correspondingly with higher temperatures, a phenomenon likely linked to the high rate of concentration via high-temperature evaporation. It should be noted that the ore-controlling factors mentioned here require further scientific statistical data for validation.

4.2.2 Involvement of mantle-derived material and its quantity

Helium isotope studies indicate (Guo, 2019) that hot springs and brines supplied by mantle-derived material exhibit higher concentrations of rare metals such as rubidium, and that the content of these rare metals rises significantly as the proportion of mantle-derived components increases.

5. Discussion

A comparison of cesium and rubidium deposits in mainland China reveals a striking fact: the two share remarkable similarities across numerous aspects, including industrial and genetic types, geological settings, and mineralization mechanisms. Furthermore, these two distinct mineral resources frequently occur in association or coexistence—such as in coal deposits and Quaternary hot springs—and both exhibit endogenic, exogenic, and superimposed (combined endogenic-exogenic) mineralization types.

Much like cesium mineralization, rubidium deposits in mainland China are predominantly associated/paragenetic minerals; no purely independent rubidium deposits have yet been discovered. Although the genetic types of rubidium deposits in mainland China are diverse—indeed, virtually comprehensive—the ore quality is generally low. Moreover, potential liquid rubidium deposits are located in remote highland areas with poor infrastructure, such as transportation networks, posing significant challenges for large-scale extraction and utilization at present.

Regarding the mechanisms of ore formation and the sources of ore-forming materials, the genesis of rubidium deposits is inextricably linked to tectono-magmatic activity, with the active participation of mantle-derived materials playing a crucial role. Even deposits that appear superficially to be entirely exogenous in origin—such as coal-hosted rubidium deposits and liquid rubidium occurrences—actually rely heavily on the involvement of mantle-derived materials and the influence of tectono-magmatic processes.

Whether concerning the rubidium mineralization discussed here or other rare metal deposits (such as those of cesium), their ultimate formation is governed by specific controlling factors. These include magmatic crystallization differentiation and hydrothermal metasomatism, the degree of magmatic differentiation, the intensity of magma melt-fluid interaction, the extent of crustal material contamination, magmatic oxygen fugacity and the remelting of crustal materials, the intensity of alteration, the participation of fluxing and incompatible elements, and the influx and quantity of mantle-derived materials; in the specific case of liquid rubidium mineralization, hot spring temperatures are also a factor.

6. Conclusions

Rubidium mineralization in mainland China is diverse and varied, encompassing nearly all known genetic deposit types found in geological textbooks—such as pegmatite, various granite-hosted, magmatic-hydrothermal, quartz and mica-hydrothermal vein, skarn, volcanic, porphyry, alkaline igneous, and crypto-explosive breccia types. There are also coal-hosted, secondary weathered granite crust, and placer deposits, as well as non-hard-rock types like Quaternary hot springs and surface or subsurface brines.

It must be noted, however, that while these rubidium deposits are diverse, their grades are generally low. Furthermore, the vast majority are located on the Tibetan Plateau and its periphery—regions characterized by poor transportation and inadequate infrastructure—meaning their development faces significant challenges, including high investment costs, harsh natural conditions, and the inevitable disruption of pristine ecosystems.

As with many other rare metal mineralization systems, the formation of rubidium deposits in mainland China is inextricably linked to active tectono-magmatic processes and the input of mantle-derived ore-forming materials. In other words, orogenesis is a crucial prerequisite for the formation of numerous rare metal deposits, including those of rubidium; even liquid-phase deposits—such as brines and/or hot springs—rely on the underlying influence of concealed tectono-magmatic activity.

7. References

01. Ban MJ, Wang L and Mao JW et al. 2025. Geological characteristics, metallogenic regularity, and prospecting significance of the Changchengling rubidium polymetallic deposit in southern Hunan. *Geotectonics and Metallogeny*, (3).

02. Chen D, Luo P and Liu GY et al. 2010. Extraordinary enrichment of rare metals (Sn, Li, Rb, Cs) and magmatic evolution at Jinjiling, southern Hunan. *Geological Review (S1)*: 4. DOI: 10.16509/j.georeview.2025.s1.042.

03. Chen ZW, Yuan C and Lin ZF et al. 2024. Genesis and rubidium enrichment mechanism of amazonite granite at Jiangjunshan, Altay, Xinjiang. *Geotectonica et Metallogenia*, 48 (6): 1394-1415.

04. Chen XF, Fan Y and Zhou TF et al. 2022. A Study on the occurrence state and metallogenic mechanism of rubidium in the Xiwukou deposit, Ningguo, Anhui Province, in the Jiangnan uplift belt. *Earth Science Frontiers*, 29 (1):16. DOI: 10.13745/j.esf.sf.2021.8.4.

05. Cheng JL, Cui ZL and Li FG et al. 2026. Characteristics and prospecting significance of phlogopite-type rubidium deposit in the Diantan skarn belt, Tengchong. *The Chinese Journal of Nonferrous Metals*, 36 (2): 626-641.

06. Du B, Li FG and Bi XL et al. 2025. A brief analysis of the geological characteristics and genesis of the rubidium deposit at Dayangtian, Tengchong, Yunnan. *Yunnan Geology*, 44 (1): 92-95.

07. Du LT.1983. Geochemical characteristics and classification of alkali-metasomatic mineralization. *Geology of Ore Deposits*, (02): 35-43. DOI: CNKI:SUN:KCDZ.0.1983-02-004.

08. Duan XZ, Tan KX and Xie YS et al. 2016. Geological characteristics and genesis of the Shihuyao granite-type niobium-tantalum-rubidium deposit in Inner Mongolia. *Geology and Resources*, 25 (1): 9. DOI：10.3969/j.issn.1671-1947.2016.01.006.

09. Fan FP, Xiao HL and Chen LZ et al. 2022. Geology, petrogenetic and metallogenic ages, and metallogenic model of the Liangyuan Nb-Ta-Rb-W deposit, northern Guangdong. *Acta Petrologica Sinica*, (02): 038.

10. Fang WX, Guo YQ and Li TC. 2024. Volcanic-intrusive rock sequences and metal mineralization in rift basins of the eastern Yunnan region. *Acta Geologica Sinica*, 98 (6): 1776-1802.

11. Guo W. 2019. Characteristics and significance of rare-metal mineralization in the hot springs of Tengchong, Yunnan. *Acta Geologica Sinica*, 93 (6): 1321-1330.

12. Hou YL. 2023. Overview of geological research on rubidium deposits in my country and implications for prospecting. *Western Exploration Engineering*, 35 (2): 117-119. DOI: 10.3969/j.issn.1004-5716.2023.02.034.

13. Kong HL, Zhang JW and Jin MS et al. 2021. Progress in the exploration of pegmatite-type critical metal deposits (lithium, beryllium, etc.) in the Northern Margin of the Qaidam Basin, Qinghai. *Proceedings of the First National Mineral Exploration Conference*.

14. Li HY, Lei L and Chai MC et al. 2025. Hydrothermal metasomatism leads to the enrichment of the rare metal rubidium in highly fractionated granitic rocks. *Journal of Guilin University of Technology*, (6).

15. Li JB. 2020. Analysis of geological characteristics and application prospects of rubidium deposits in Dongkeng mining area, Jianning County, Fujian Province. *Nonferrous Metals Abstracts*, 35 (05): 34-38.

16. Li JL, Liu Q and Xu LB et al. 2015. A brief analysis of the geological characteristics and genesis of the Shimen rubidium deposit in Songxian County, Henan Province. *Mineral Resources and Geology*, 29 (2): 5. DOI: CNKI:SUN:KCYD.0.2015-02-012.

17. Li L, Xia Y and Zhou QM et al. 2024. Study on ore characteristics and rubidium occurrence modes of the Xianglushan rubidium deposit in the Yuechengling area, Guangxi. *Mineral Resources and Geology*, 38 (1): 98-105.

18. Li XF, Xu H and Zhu YT et al. 2025. Metallogenic regularities and prospecting directions for rare metal deposits in Western Yunnan. *Acta Petrologica Sinica*, (7).

19. Liang CF, Han B and Wu LW et al. 2025. Geological characteristics and genesis of rare polymetallic deposits such as rubidium in Abudartai, Siziwang Banner, Inner Mongolia. *Geology and Resources*, 34 (4): 410.

20. Liu HW, Lei AQ and Liu CC. 2010. Geological characteristics and genesis of the Tuanbaoshan feldspar-rubidium deposit in Qinghai Province. *Western Exploration Engineering*. DOI: CNKI: SUN:XBTK.0.2010-07-045.

21. Liu XH. 2023. *Mineralogy, Geochemistry, and Metallogenesis of the Zhengchong Rubidium-Polymetallic Deposit, Dao County, Hunan Province*. Doctoral dissertation, Central South University.

22. Qin YL, Xu YF and Zhan HY et al. 2024. Geological characteristics and prospecting direction of the Changzheng Yalakan granite-pegmatite type rubidium deposit in Daofu County, Sichuan. *Acta Geologica Sichuanica*, 44 (3): 422-427.

23. Sha XB. 2026. *Study on Mineralization Types and Element Association Characteristics of the Jiajika Rare-Metal Ore Field in Western Sichuan*. Doctoral dissertation, Chengdu University of Technology.

24. Shen ZJ, Xie LL and Lin ZY. 2003. Characteristics of major rare earth metal deposits in Hunan Province. *Hunan Geology*. DOI: CNKI:SUN:HNDZ.0.2003-01-006.

25. Sun Y. 2013. *Study on Typical Rubidium Deposits and Their Metallogenic Tectonic Settings in my country*. Doctoral dissertation, China University of Geosciences, Beijing.

26. Sun Y, Wang DH and Wang CH et al. 2019. Metallogenic regularities, new progress, and prospecting directions for rubidium deposits in my country. *Acta Geologica Sinica*. DOI: CNKI:SUN:DZXE.0.2019-06-005.

27. Sun Y, Wang RJ and Li JK et al. 2015. ^{40}Ar-^{39}Ar dating of muscovite and analysis of prospecting potential for the Shihuiyao Rb-polymetallic deposit, Xilinhot. *Geological Review*, 61 (2): 463-468.

28. Sun Y, Wang RJ and Qi F et al., 2013. Current status of global rubidium resources and suggestions for rubidium development and utilization in my country. *China Mining Magazine*, 22 (9): 4. DOI: 10.3969/j.issn.1004-4051.2013.09.003.

29. SunYZ, Zhao CL and Wang JX et al. 2017. A method and process for separating and extracting rubidium and cesium from coal. Document ID: 12940873 (in Chinese). https://www.xjishu.com/zhuanli/24/201710615317.html. Retrieved June 8, 2026.

30. Tang GQ and Wu CZ. 2024. Main genetic types and metallogenic potential of hard-rock rubidium deposits in Xinjiang. *Bulletin of Mineralogy, Petrology and Geochemistry*, 43 (1): 102-126. DOI: 10.3724/j.issn.1007-2802.20240007.

31. Wang J. 2009. Report on the General Survey (Interim) of Rare Metal Deposits in the Nading Mining Area, Cona County, Tibet Autonomous Region. The Sixth Geological Brigade, Bureau of Geology and Mineral Exploration and Development of Tibet Autonomous Region.

32. Wang YG, Li J and Tian Y et al.2020. Geological characteristics and genesis of the Chaharihada rubidium-rare metal deposit in the Yuanbaoshan Area, Beishan Region. *China Mining Magazine*, 29 (S01): 5. DOI: 10.12075/j.issn.1004-4051.2020.S1.085.

33. Wang YS，Guo J and Liu XF et al. 2024. Research on rubidium and cesium resources, extraction technologies, and development and utilization in China. *Acta Geoscientica Sinica*, 45 (5): 823-829. DOI: 10.3975/cagsb.2024.072401.

34. Wang YT, Du JG and Lei RX et al. 2024. Characteristics of ore-forming fluids and mineralization processes of cryptovolcanic breccia-type lithium-rubidium ore bodies in the Weilasto deposit, Inner Mongolia. *Earth Science-Journal of China University of Geosciences*, 49 (12): 4318-4318 DOI: 10.3799/dqkx.2024.054.

35. Wang ZY, Xiao SG and Sun CW et al. 2025. Geological characteristics and prospecting potential of a newly discovered granite-hosted lithium-rubidium deposit in Gejiu, Yunnan. *Advances in Geosciences*, 15 (1): 94-103. DOI: 10.12677/ag.2025.151011.

36. Wen CH, Chen JF and Sun J et al. 2024. Prospecting model and prospecting directions for granite-type lithium-rubidium-niobium-tantalum deposits in Hunan Province. *Land and Resources Guide*, (4): 1-16.

37. Wu CZ, Jia L and Lei RX et al. 2021. Main characteristics and research progress of amazonite granites and associated rubidium deposits in the Central Asian orogenic belt. DOI: 10.18654/1000-0569/2021.09.02.

38. Xiao SG, Chang GH and Wang ZY et al. 2024. The first granite-type lithium-rubidium deposit has been discovered in Gejiu, Yunnan. *Mineral Resources and Geology*, 38 (1): 205-206.

39. Xie JL, Lin B and Qi J et al. 2023. Research progress on granite-type rubidium deposits and prospecting directions for rubidium deposits in the Qinghai-Tibet Plateau. *Gold Science and Technology*, 31 (1): 26-36.

40. Xie JL, Tango JX and Lin B et al.2025. Zircon U-Pb age and occurrence of rubidium in the Gari'atong super-large granite-hosted rubidium deposit, Tibet. *Acta Geologica Sinica*, 99 (8): 2724-2738.

41. Xing P. 2020. *Fundamental Research on the Comprehensive Utilization of Granite-Type Rubidium Ore Resources*. Doctoral dissertation, University of Science and Technology Beijing.

42. Xu F, Song GS and Wang MZ et al. 2016. Geological characteristics and prospecting potential of the Ziyugou pegmatite-type rubidium deposit in Danfeng, Shaanxi Province. *Geology and Mineral Resources of South China*, 32 (1): 9. DOI: 10.3969/j.issn.1007-3701.2016.1.008.

43. Xue Z, Zhang WS and Gao F et al. 2020. Geological characteristics of mineralization and prospecting targets for greisenized granite (used for ceramics) and rubidium deposits in Maishi, Tongcheng County, Hubei Province. *Resources, Environment & Engineering*. DOI: 10.16536/j.cnki.issn.1671-1211.2020.S1.002.

44. Yang F. 2017. Geological characteristics and genesis of the Dongkeng rubidium deposit in Jianning, Fujian. 36 (8). DOI: CNKI:SUN:FJDZ.0.2017-03-007.

45. Yi M. 2025. Uranium, rubidium, gold: major breakthroughs achieved in strategic metal exploration. Hebei Geology, (3): 38.

46. Yin JZ. 2026c. Type and origin of the gallium deposits in Mainland China. *Naturalis Scientias*, 3: 662-675. DOI: https://doi.org/10.62252/NSS.2026.1037.

47. Yin JZ. 2026d. Geology and geochemistry of the germanium deposits in Mainland China. *Naturalis Scientias*, 3: 686-709. DOI: DOI: https://doi.org/10.62252/NSS.2026.1039.

48. Yin JZ. 2026e. Genetic types and geology of cesium deposits in Mainland China. *Naturalis Scientias*, 3: 739-762. DOI: https://doi.org/10.62252/NSS.2026.1041.

49. Yin JZ, Li KN and Shi HY et al. 2025. Mathematical, physical, and chemical interpretations of structural control and contributions to gold mineralization. Preprints ID: 202501.1183. DOI: 10.20944/preprints202501.1183.v1.

50. Yu JS, Li Q and Zhou X et al. 2019. Geological characteristics and prospecting potential of the Jianong niobium-tantalum-rubidium deposit in Basu County, Eastern Tibet. *World Nonferrous Metals.*

51. Yuan TJ. 2026. *Study on the Geological and Geochemical Characteristics and Ore-Bearing Potential of Granites in the Jiajika Mining Area, Sichuan*. Doctoral dissertation, Chengdu University of Technology.

52. Zhang D. 2019. *A Preliminary Study on the Geochemical Characteristics and Mineralization of Rubidium-bearing Granites and Pegmatites in the Xingxingxia Area, Beishan*. Doctoral dissertation, Lanzhou University.

53. Zhao W. 1987. Pilot-scale study on the extraction of potassium, barium, rubidium, and cesium from gas field water in a certain area. *Collected Papers of the Chinese Academy of Geological Sciences (15)*.

54. Zhu ZY, Kong FC and Wang JP et al. 2025. Distribution patterns and enrichment mechanisms of lithium, rubidium, and cesium in the hot springs of Bukadaban Peak, Hoh Xil. *Acta Petrologica Sinica*, (3).

Data availability

The data that support the findings of this study are available from the author upon reasonable request.

Declaration of competing interest

The author declares that he has no competing financial interests or personal relationships that could have appeared to influence the work reported in this paper.

Use of AI tools declaration

The author declares that he has not used Artificial Intelligence (AI) tools in the creation of this article.